On the Detection of Chemically-Induced Hot Electrons in Surface Processes: from X-ray Edges to Schottky Barriers†

J. W. Gadzuk

National Institute of Standards and Technology, Gaithersburg, Maryland 20899

Received: March 14, 2002

The potential involvement of electron−hole pair excitations in atomic/molecular processes such as sticking/adsorption/dissociation at metal surfaces has long been debated, particularly by those previously involved with similar issues in electron spectroscopies of localized core levels in solids. Recent experiments have detected hot electrons produced as various gases were adsorbed on a thin metal film that formed a Schottky barrier with an n-type Si substrate upon which the film was deposited. Drawing upon analogies with spectroscopic processes leading to the X-ray edge singularity, a theoretical model for the electronically nonadiabatic effects is presented here that accounts for the observed hot electron production.

1. Introduction

The role of substrate conduction band electron−hole pair excitations in fundamental surface processes such as sticking, molecular dissociation, adsorption, inelastic beam scattering, etc. was frequently questioned/raised in "modern terms" throughout the decade of the 70s and early 80s.[1−9] Many of these studies focused on phenomena in which charge transfer between an incident particle and the surface was a defining characteristic of the process.[10−14] The motivation was at least in part due to perceived similarities between a dynamic charge-transfer event involving the massive incident particle interacting with the electron−hole pair continuum of the substrate and the related ionization (and thus "charge transfer") that occurred in X-ray absorption and/or photoelectron spectroscopy of core levels. In both cases, the electron−hole pairs see a transient switching on of a localized atomic-like potential (the difference between the potential of the initial neutral and the charged particle). This dynamic potential, similar in both cases, excites electron−hole pairs. A considerable expertise had been developed to deal with these issues in core-level-spectroscopy.[15−25] It was a natural next step for these "experts" to also consider the connections between atom scattering/sticking at metal surfaces and electron−hole pair excitations. A particularly intriguing point was raised by the Anderson Orthogonality Theorem (AOT) which demonstrates that the many body ground state of an infinite Fermi system/electron gas is orthogonal to the ground state of the same system within which a localized potential has been introduced.[15] One consequence of the AOT is that the permanent switching on of a potential in an electron gas always results in excitation of electron−hole pairs, with zero-probability for perfectly elastic switching, independent of the details of the switching process. Thus, truly adiabatic processes in such systems are rigorously impossible, no matter how slowly they proceed. This has lead many to wonder whether such effects have been observed? Although the phenomenon of exoelectron emission accompanying an exothermic chemical process at a surface has been well-known and documented for many years,[13,26−32] this observable manifestation of electron−hole pair excitation has still failed to put to rest within the surface science community the question of whether incontrovertible direct evidence exists supporting the involvement of electron−hole pair excitation.

It is within this historical context that a recent series of papers[33−36] on the general topic of "chemically induced electronic excitations at metal surfaces" has both raised current interests[37] and also stimulated in depth retrospective studies on the problem of electron−hole pair excitation and detection in surface processes.[38,39] These studies are based on an extension of the elementary exoemission phenomenon in which hot electrons produced with energy in excess of φ, the work function of the surface, are in principle observable in traditional exoelectron configurations. Because φ is typically several electronvolts, the yield of exoelectrons produced in an $\lesssim$1 eV exothermic event is too small to be dependably useful. The Santa Barbara group recognized that if the reaction occurred on the surface of the same metal, now prepared as an ∼50−100 Å thin film deposited on an n-type semiconductor (Si) thereby forming a Schottky diode, the same distribution of exoelectrons would be initially produced as on the extended metal. However, a significant fraction of the hot electrons directed inward will arrive at the Schottky barrier. Since now the barrier heights are only several tenths of an eV, a large percentage of the exoelectrons will transmit into the Si conduction band and be measurable as a "chemically induced reverse diode current, a chemicurrent".[36] This is a time-reversed realization of a family of hot-electron processes in metal−insulator-thin metal junctions shown in Figures 1a−c in which electrons tunnel from the substrate into the junction side of the thin metal film, cross the thin film in an outward trajectory, and then: emit into vacuum (a cold cathode electron beam source)[40,41] [Figure 1a]; excite surface plasmons at the outer metal-vacuum interface, which then radiate[42,43] (Figure 1b); undergo inelastic resonance scattering from an adsorbate, a bond-selective excitation/reaction process that is sometimes referred to as Hot Electron Femtochemistry at Surfaces (HEFatS)[44,45] (Figure 1c). Useful similarities exist between these hot-electron surface processes involving M−I−M tunnel junctions and those occurring in Ballistic Electron Emission Spectroscopy (BEEM) constructions shown in Figure 1d, in which a scanning tunneling microscope (STM) tip injects hot electrons at the vacuum-metal interface of a thin film Schottky diode.[46−48] This is also exactly what

† Part of the special issue "John C. Tully Festschrift".

10.1021/jp025761y
Published on Web 06/14/2002

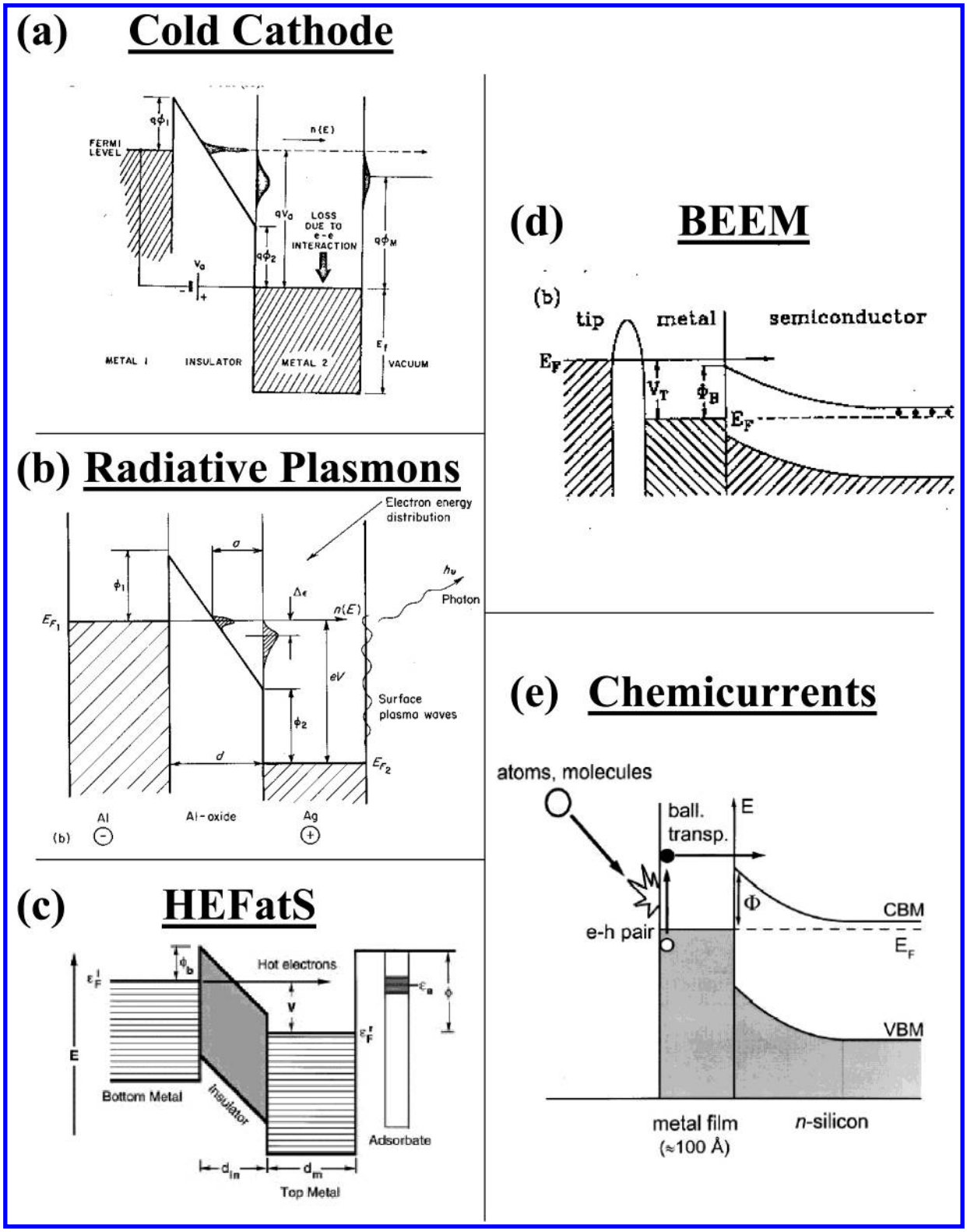

Figure 1. Hot electron applications using junctions. Left column: metal−insulator-metal sandwiches. Right column: Schottky barrier devices. (a) Cold cathode electron source (ref 41). (b) Radiative surface plasmon excitation and decay (after refs 42 and 43). (c) Resonant hot electron scattering from adsorbates (ref 44). (d) Ballistic electron emission microscopy (ref 47). (e) Chemically induced hot electron detector (ref 36).

happens in the "chemicurrents" detector[33−36] but with the reactive event symbolized by the starburst in Figure 1e, rather than the STM tip serving as the source of hot electrons. Otherwise, the phenomenology is the same and this realization has provided a useful starting point for theoretical model building.

The present note appeals to existing knowledge from complimentary areas that can serve as a basis for understanding. In particular, the limited issue of why and how much "chemicurrent" can reasonably be expected will be addressed, drawing upon that which is already known from past experience involving core level spectroscopies,[15−25] driven bosonized Fermi systems,[49−51] and various tunneling devices.[40−48] Guidance will be provided for estimating the chemicurrent yield that is produced in an adsorption/sticking event without fully addressing the more complete problem of what is the dominant

dissipative mechanism responsible for the sticking: electron−hole pairs, phonons, internal molecular degrees of freedom, entropy,etc. Aspects of this are taken up in the more inclusive study.[39] In Section 2, the basic results drawn from electron−hole pair excitation in core level spectroscopies,[15−25,49] hot-electron transport in tunnel junctions,[40−45] and Schottky barrier "spectroscopy" in BEEM[46−48] will be brought together, providing a compact description of the essential features in the chemicurrent phenomena. Some illustrative (computationally nonintensive) numerical implications are next presented and final discussion then offered.

2. Chemicurrent Model

One can exploit the common features of the following: the M−I−M devices in which hot electrons are introduced into the thin film via a tunneling mechanism, as displayed in Figure 1a−c; the (time-reversed) BEEM construction, in which an STM tip injects hot electrons into the thin metal film as depicted in Figure 1d; and the chemically induced electronic excitation detector of Figure 1e in which the exothermicity of the surface "reaction" is transferred, at least in part, to electron−hole pair excitations at the vacuum-thin metal film interface. In all of these cases, the total process is reasonably represented as a sequential, independent multistep process of the following: (i) hot electron injection into the metal film; (ii) hot-electron transport with attenuation across the thin metal film; (iii) energy-dependent transmission over/through the Schottky barrier in BEEM and chemicurrent detection or inelastic resonant scattering from adsorbates in HEFatS. Step (ii) is identical in BEEM and chemicurrents as well as in all the M−I−M devices, as discussed elsewhere.[39,45] A form of the independent three-step model which is useful in BEEM and chemicurrent applications gives the injected current passing over the Schottky barrier as the integrated product

$$I_B = \int_{-\infty}^{+\infty} d\epsilon_{in} \int_{2\pi} \int d\Omega\, j_o'(\epsilon_{in},\hat{u}) T_{l-r}(\epsilon_{in},\hat{u}) C(\epsilon_{in},\hat{u}) \quad (1)$$

where the integration is performed over electron energy ϵ_{in} and direction defined by the unit vector $\hat{u}$ and solid angle segment $d\Omega$. In eq 1, $dj_o(\epsilon_{in}, \hat{u})/d\epsilon_{in} \equiv j_o'$ is the possibly angle-dependent source energy distribution of the injected hot electrons within which density of states (DOS) factors have been included. For the BEEM scenarios, j_o' is obtained from standard STM theory[55,56] and for chemicurrent detection, which is the topic of this study, from the "X-ray edge model" to be discussed in section 2.2.[16,17] $T_{l-r}(\epsilon_{in}, \hat{u})$, a transfer function through the thin metal film, accounts for the effects of both primary beam attenuation and also secondary electron generation. $C(\epsilon_{in}, \hat{u})$, the transmission coefficient across the metal-semiconductor interface, can be as simple as a unit-step function for $\epsilon_\perp \geq \phi_b$ or as complex as that which emerges from a full scale electronic structure calaculation.[52,53] For present purposes, "simple" will be fine.[54]

2.1 Attenuation. The product $j_o'(\epsilon_{in})T_{l-r}(\epsilon_{in}) \equiv j_b'(\epsilon_{in})$ in eq 1 is the energy distribution of the current incident upon the Schottky barrier (or metal-vacuum interface in HEFatS) from the metal film. Due to the continuum of electron−hole pair excitations within the metallic thin film, the primary electron flux is attenuated by an exponential factor $T_o(\epsilon_{in},\hat{u}) \approx \exp(-d(\hat{u})/\lambda(\epsilon_{in}))$ where $d(\hat{u})$ is the ballistic electron path length through the film and $\lambda(\epsilon_{in})$ is the attenuation length. The venerable theory of Quinn[57] provides a still-credible expression which, in its simplest low-energy form, is

$$\lambda(\epsilon_{in}) \cong \chi(r_s)(1 + \epsilon_{in}/\epsilon_{Fermi})^{1/2}/\epsilon_{in}^2 \quad (2)$$

with the material-dependent $\chi(r_s) \approx 10\,500/r_s^{7/2}$eV^{2}Å, $\epsilon_{Fermi} \approx 50/r_s^2$eV, r_s is the usual Fermi system electron density parameter, and ϵ_{in} specified with respect to a zero at the Fermi level. Taking Al(Cu) with $r_s \approx 2(2.7)$ as examples, $\lambda(\epsilon_{in} = 2\text{ eV}) \approx 250(100)$ Å.

Strictly speaking, the secondary electron cascade generated by the primary beam should be included, as detailed in BEEM[47] and HEFatS[45] applications. However, since $\epsilon_{in} \leq 2$ eV for the chemicurrent realizations of interest so far, $\lambda(\epsilon_{in}) \geq 100$ Å which, with $d < 100$ Å, suggests that the incident current due to secondaries with energy greater than φ_b but less than ~2 eV will be small[45] and thus can be neglected here.

2.2 Excitation. If a potential is suddenly switched on within an extended electron gas/Fermi system, then in the long-time limit, the electron-gas is necessarily raised to an excited-state according to the distribution

$$P(\omega) = |\langle V_{loc};\epsilon = \hbar\omega|0;0\rangle|^2 \quad (3)$$

where $|V_{loc};\epsilon\rangle$ and $|0;0\rangle$ are many body excited and ground states with and without the localized potential. In this form, $P(\omega)$ given by eq 3 plays the role of a many-body Franck−Condon factor. If the potential is a localized atomic-like potential such as that from a suddenly created core hole, then the excitation probability distribution falls under the generic heading of the Mahan−Nozières−de Dominicis (MND) X-ray edge divergence[16,17] about which much has been written.[15−23,58,59] Without going into great detail, the idea is that many low energy pairs can be produced, in analogy with discrete atomic shake-up, upon localized hole creation, and this transforms the absorption-threshold into a divergent-but-integrable form which ND solved exactly in the long-time limit (i.e., right at threshold) as

$$P(\omega) = N\frac{1}{\omega^{1-\alpha}}\,(0 < \omega < \omega_c = \epsilon_c/\hbar) \quad (4)$$

where $N = \alpha/\omega_c^{\alpha}$ is a normalization (per unit energy) factor, ϵ_c a cutoff energy of order the conduction bandwidth, and $\alpha \approx (\delta/\pi)^2 \leq 0.25$, where δ is the dominant Fermi-level electron phase shift associated with the localized hole potential. A similar expression can be obtained for a localized potential outside a metallic surface,[6,9,25] in which case α and ω_c become functions of the hole-surface separation.[25,60] The main point to be stressed here is the inherent identity between the overlap integrals, the electron−hole pair excitation spectrum, and the electron-gas Franck−Condon factors.

Although the sudden-limit provides useful guidelines and also an upper limit to the distribution of excited states produced, a softer introduction of the localized potential into the Fermi system might be expected when thermal beams of atoms or molecules are incident upon a surface, as in the chemicurrent studies.[33−37] In the comprehensive theory of the dynamic response of the electron gas to such potentials by Müller-Hartman et al., the influence of the switching rates is considered.[49] In contrast to the sudden-on case (eq 4), they find that the distribution of excited electron−hole pair states generated by the same localized potential that is exponentially rather than suddenly switched on ($V(t) \approx V_o \exp(+\eta t)$, $-\infty < t < 0$; $=V_o$, $t \geq 0$) is

$$P(\omega) = \frac{e^{-\omega/\eta}}{(\Gamma(\alpha)\eta^{\alpha})\omega^{1-\alpha}} \quad (5)$$

which redistributes weight from the high-energy tail (where $\omega > \eta$) back into the low-energy region. Essentially, this form of

spectrum guarantees that there will be no Fermi system response until the perturbation is acting. Intuitively, one expects $1/\eta$, the characteristic time scale, to be of the order of Δx/vel, where Δx is the width of the region outside the surface within which the potential switches ($0.1 \lesssim \Delta x \lesssim 1$ Å) and vel $\simeq (2D/M)^{1/2} \simeq 1.4 \times 10^{14} D^{1/2}/Z$ Å/sec is a typical velocity in this region (D = potential well depth or adsorption energy in eV and Z = mass number). The switching region is where the particle-surface interaction changes significantly over a narrow spatial range such as at a curve crossing or seam for a charge-transfer process.[3−14, 61−72] For reasonable choices of system-defining parameters, $\hbar\eta$ falls in the range $0.1 \text{ eV} \lesssim \hbar\eta \lesssim 1.0$ eV. More extensive and rigorous considerations are taken up elsewhere.[6,39,49,50]

Finally, a connection must be made between the energy distribution of excited pairs given by eq 5 and the resulting hot-electron source function $j_o'(\epsilon_{in}, \hat{u})$ required in eq 1 for the Schottky junction current that is the hoped-for signature of the exothermic "chemical event" responsible for the electron−hole pair excitation in the first place. The reality is that a hot electron with energy ϵ_{in} may have been part of any of a continuum of single or multiple electron−hole pairs with total energy within the range $\epsilon_{in} \lesssim \hbar\omega \lesssim \epsilon_{in} + \epsilon_{Fermi}$. In its most elementary formulation, the excited pair distribution given by eq 5 derives from a Golden-Rule type of expression requiring integration over all exclusion-principle-allowed electron and hole states. In the limiting case of single-pair excitation

$$P_{e-h}(\omega) = \int_{\epsilon_o<\epsilon_{Fermi}\,\epsilon_{in}>\epsilon_{Fermi}} \rho(\epsilon_o)\rho(\epsilon_{in}) \times \delta(\epsilon_o + \hbar\omega - \epsilon_{in})|V(\omega)|^2 d\epsilon_o d\epsilon_{in} \quad (6)$$

Equation 6 expresses the fact that a pair state at energy $\hbar\omega$ is a superposition of electron and hole states with energies above (ϵ_{in}) and below (ϵ_o) the Fermi level (each with a density of states $\rho(\epsilon)$), having been excited by V(ω), the ω'th Fourier component of a suitably defined transient potential. As discussed at great length by Müller-Hartmann et al.,[49] simple phase space considerations show that when $\hbar\omega \lesssim \epsilon_{Fermi}$, the pair DOS is well represented by $\rho_{e-h}(\omega) \approx \rho^2(\epsilon_{Fermi})\,\hbar\omega$ where $\rho(\epsilon_{Fermi})$ is the actual electron DOS at the Fermi level. This simplification reduces eq 6 to

$$P_{e-h}(\omega) \approx \rho^2(\epsilon_{Fermi})\hbar\omega|V(\omega)|^2 \quad (7)$$

which when equated with eq 5, provides an expression for $|V(\omega)|^2$ that is consistent with the X-ray edgeology. The hot-electron energy distribution that is implied by eq 6 is

$$\frac{dP(\epsilon_{in})}{d\epsilon_{in}} = \rho(\epsilon_{in})\int_{\epsilon_{in}}^{\epsilon_{in}+\epsilon_{Fermi}} \rho(\epsilon_{in} - \hbar\omega)|V(\omega)|^2 d(\hbar\omega) \quad (8)$$

which, upon setting both electron DOS $\approx \rho(\epsilon_{Fermi})$, taking the upper limit to infinity, and using eqs 5, 7, and 8, becomes

$$\frac{dP(\epsilon_{in})}{d\epsilon_{in}} \cong \frac{1}{\hbar\Gamma(\alpha)\eta^\alpha}\int_{\epsilon_{in}}^{\infty} \frac{e^{-\omega/\eta}}{\omega^{2-\alpha}} d\omega = \frac{1}{\hbar\eta}\frac{\Gamma(-1+\alpha,\epsilon_{in}/\hbar\eta)}{\Gamma(\alpha)} \quad (9)$$

Hot electron energy distributions obtained from eq 9 for a range of localized potential strengths, as embodied in the magnitude of their phase shifts hence α values, are shown in Figure 2. Clearly, the switching rate η sets the upper energy limit of the phenomena. For given η, the stronger the potential, the greater is the probability of hot electron production. Both consequences are in accord with intuitively based expectations.

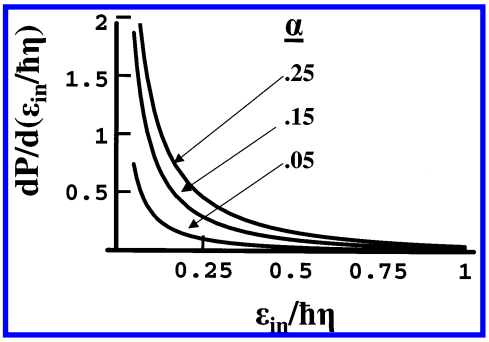

Figure 2. Hot electron energy distribution (eq 9) per incident particle as a function of energy above the Fermi level, in units of $\hbar\eta$ for a range of potential strengths, as conveyed by α.

2.3 Current/Yield. A workable expression for the total chemicurrent through the Schottky diode can now be deduced from eqs 1, 2, and 9 and a few noncrucial specifications that facillitate the solid angle integration. As already mentioned, the role of $C(\epsilon_{in},\hat{u})$ in the unit-step-function-approximation, is to impose limits on the θ integration such that $(\varphi_b/\epsilon_{in})^{1/2} \le \cos\theta \le 1$. Within the range of θ of relevance here, the transfer or attenuation factor (neglecting secondary electrons) is well represented as

$$T_{l-r}(\epsilon_{in},\hat{u}) = \exp(-d/(\lambda(\epsilon_{in})\cos\theta)) \approx \exp(-d(1 + \theta^2/2 + ...)/\lambda(\epsilon_{in}))$$

For an isotropic s-wave hot-electron source, $j_o'(\epsilon_{in},\hat{u}) = \nu_{surf}\,dP(\epsilon_{in})/d\epsilon_{in}$, where ν_{surf} is the arrival rate of atoms or molecules incident upon the surface. Consequently, the solid angle integration in eq 1 is

$$I_\theta \equiv \int_0^{\theta_{max}} \sin\theta \times \exp(-\theta^2 d/2\lambda) d\theta = \frac{\lambda}{d}(1 - \exp(-\theta_{max}{}^2 d/2\lambda))$$

with $\theta_{max} = \cos^{-1}(\varphi_b/\epsilon_{in})^{1/2}$. Because the additional energy of the hot electrons above the Fermi level is a small fraction of ϵ_{Fermi}, from eq 2, $\lambda(\epsilon_{in}) \approx \chi(r_s)/\epsilon_{in}{}^2$. The end result is that $Y(\alpha,\eta,\epsilon_{max}) = I_b/v_{surf}$, the chemicurrent yield per incident particle that sticks, is

$$Y(\alpha,\eta,\epsilon_{max}) \cong \frac{\chi}{\hbar\eta\Gamma(\alpha)d}\int_{\varphi_b}^{\epsilon_{max}} d\epsilon_{in}\Gamma(-1+\alpha,\epsilon_{in}/\hbar\eta) \times \frac{\exp(-\epsilon_{in}{}^2 d/\chi)}{\epsilon_{in}{}^2}(1 - \exp(-\epsilon_{in} d(\epsilon_{in} - \varphi_b)/2\chi)) \quad (10)$$

where ϵ_{max} is the total amount of energy that can be delivered to the electronic excitations, or in otherwords, the sum of the well depth of the adsorption bond plus whatever kinetic and internal energy the incident particle brings to the surface.

3. Results

At this point, some characteristic numerical consequences of this exercise will be put forth. On the basis of the hot-electron energy distribution shown in Figure 2, the integrand in eq 10 will be significant mainly for $\epsilon_{in} \le \hbar\eta$. Obviously, this requires $\varphi_b \ll \hbar\eta$ which just says that the switching on rate (and as a result the nonadiabaticity) of the localized potential must be fast enough to excite electrons with energy in excess of the Schottky barrier. It was suggested that $\eta \approx D^{1/2}$ and $\epsilon_{max} \approx D$.

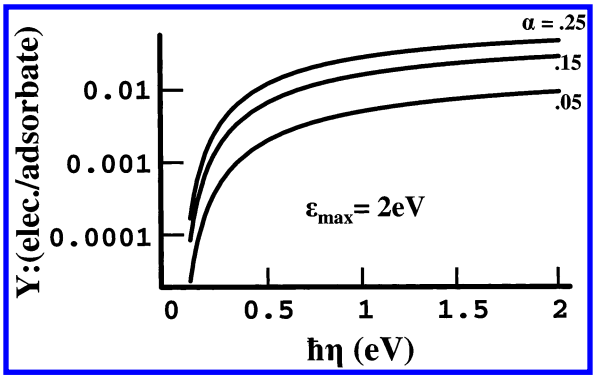

Figure 3. Initial chemicurrent yield (# electrons per incident adsorbate) vs $\hbar\eta$ in eV, from eq 10, for Schottky detector characterized by $r_s \approx 2$, $d \approx 100$ Å, $\varphi_b = 0.25$ eV. The process parameters are $\epsilon_{max} = 2$ eV and $\alpha = 0.05$, 0.15, and 0.25, as labeled.

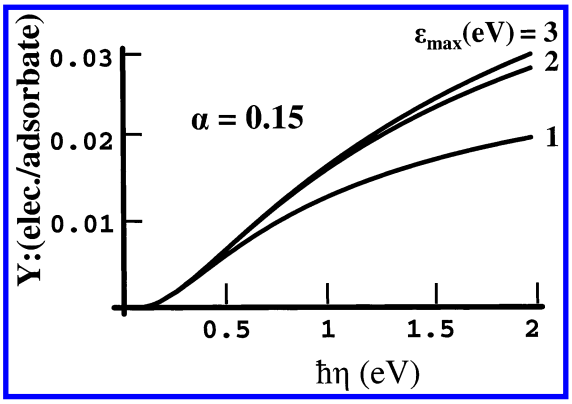

Figure 4. Initial chemicurrent yield (# electrons per incident adsorbate) vs $\hbar\eta$ in eV, from eq 10, for Schottky detector characterized by $r_s \approx 2$, $d \approx 100$ Å, $\varphi_b = 0.25$ eV. Various values of ϵ_{max} for process parameters and $\alpha = 0.15$, as labeled.

Both of these dependencies as well as that in which more strongly interacting adsorbate−substrate systems implies larger α, lead one to expect the largest characteristic yields for the most strongly bonded complexes, as is observed experimentally (see Figure 3 in ref 36).

The chemicurrent yield (called the "initial electron detection sensitivity per incident reactant" by Nienhaus and co-workers) obtained from eq 10 is displayed in Figures 3−5. In all cases, the detector parameters have been chosen as $\varphi_b = 0.25$ eV, $d \approx 100$ Å, and $r_s \approx 2$ so $\chi(r_s) \approx 1000$ eV^2 Å and thus $d/\chi \approx 0.1$ eV^{-2}. Nominal changes in these parameters do not lead to any qualitatively interesting differences from the results reported in Figures 3−5. Figure 3 shows the chemicurrent yield as a function of the switching rate for a set of scattering strengths α and Figure 4 the same but for a range of maximum excitation energies. For switching rates in the very reasonable $\hbar\eta \approx 0.1$−0.5 eV range and with a not-extreme choice of interaction strengths α, the chemicurrent yield or "initial sensitivity per incident particle" shown here are in excellent accord with the $\sim 10^{-3}$−10^{-2} values reported by Gergen et al.[36] for the strongly interacting systems of NO_2, H, and O on Ag. It is reassuring to note that the curves in Figure 4 with $\epsilon_{max} = 1$, 2, and 3 eV are fairly insensitive to the choice of ϵ_{max} as long as $\eta < \epsilon_{max}$. This of course is a consequence of the incomplete gamma function and exponential in the hot electron distribution shown in Figure 2, part of the integrand of eq 10, which has cut off the integral long before ϵ_{max} was reached. This point is illustrated more directly in Figure 5 where the yield is shown as a function of the maximum available energy treating the switching rate

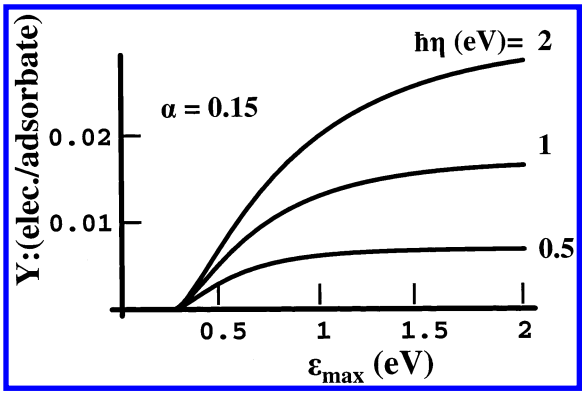

Figure 5. Initial chemicurrent yield vs ϵ_{max} with $\alpha = 0.15$ and with various switching rates η, as labeled.

parametrically. In all cases, the yields begin to saturate as ϵ_{max} exceeds η, the nonadiabaticity factor.

4. Summary

The problem of chemically induced hot electron production and detection has been addressed. Attention here has been focused on the determination of the initial electron yield per atom or molecule adsorbed on a metal surface, as recently measured and reported by Neinhaus and co-workers[33−36,38] using a detector in which the active metal surface is at the metal-vacuum interface of a thin-metal film deposited on an n-type Si surface. The model presented here has utilized knowledge developed in a number of different areas of inquiry. Excitation of metal electron−hole pairs by transient surface processes[1−9] under study has been likened to similar excitaion, widely considered in core-level spectroscopies.[15−25] In times past, useful analogies between the pair excitations leading to the socalled MND X-ray edge[16−20] in spectroscopy and the pair excitations created in nonadiabatic atom scattering and/or sticking at surfaces have provided new insights into the role of electron−hole pairs in surface dynamics.[1,6,9,49] These analogies have been invoked in the present study, providing the connection between a specified transient driving force on the substrate electrons and the resulting distribution of excited hot electrons.

Parenthetically, note that although no explicit mention of the currently very popular use of electronic friction[2,73−81] has been made here, most friction theories ultimately require the time-derivative of a Fermi-level phase shift associated with the transiently introduced potential/particle as the crucial process-defining ingredient. In the present formulation, $\alpha \Rightarrow (\delta/\pi)^2$ and η, the switching-on rate, bring the same physical content into the problem; so it seems quite likely that there is a greater essential commonality between the two approaches than one might at first guess.

Knowing the initial distribution of hot electrons, the remainder of the problem, transport from an electron "point source" across a thin film and over a Schottky barrier (Figure 1e) is identical to that encountered in various M−I−M junctions (Figure 1a−c) and in BEEM (Figure 1d). Theory developed in these areas has been immediately applicable to the problem at hand. A final expression has been obtained (eq 10) for the chemicurrent yield per adsorbed particle as a function of the interacting adsorbate−substrate parameters α, ϵ_{max}, and η and the "detector" parameters r_s (hence χ), d, and φ_b. For realistic choices $\alpha \approx 0.05$−0.1, $\epsilon_{max} \approx D \approx 1$−4 eV, and $\hbar\eta \approx 0.1$−0.5 eV, the calculated initial electron yields per adsorbate are in the $\sim 10^{-3}$−10^{-2} range which is amazingly close to the reported observations for NO_2, H, O (with adsorption energies ~2, 3, and 4 eV respectively)

on Ag.[37] The fact that these results were obtained without gratuitous squeezing of parameter choices adds support to the credibility of the model. Soon-to-be-reported[39] extensions of the model will include full scattering (in-time delay-out) processes so that issues such as "to stick or not to stick" (and how will this show up in the chemicurrent detector) can be addressed.

Acknowledgment. I would like to thank Mark Stiles for useful suggestions and feedback on matters related to this paper and John Tully for helping to make the world of chemical physics and surfaces a more decent place to live.

References and Notes

(1) Müller-Hartmann, E.; Ramakrishnan, T. V.; Toulouse, G. *Solid State Comm.* **1971**, *9*, 99.
(2) d'Agliano, E. G.; Kumar, P.; Schaich, W.; Suhl, H. *Phys. Rev. B* **1975**, *11*, 2122.
(3) Blandin, A.; Nourtier, A.; Hone, D. W. *J. Phys.(Paris)* **1976**, *37*, 369.
(4) Kasemo, B.; Törnqvist, E.; Nørskov, J. K.; Lundqvist, B. I. *Surface Sci.* **1979**, *89*, 554.
(5) Brako, R.; Newns, D. M. *Solid State Comm.* **1980**, *33*, 713.
(6) Gadzuk, J. W.; Metiu, H. *Phys. Rev. B* **1980**, *22*, 2603.
(7) Schönhammer, K.; Gunnarsson, O. *Phys. Rev. B* **1980**, *22*, 1629; Schönhammer, K.; Gunnarsson, O. *Phys. Rev. B* **1981**, *24*, 7084.
(8) Nørskov, J. K. *J. Vac. Sci. Technol.* **1981**, *18*(2), 420.
(9) Gadzuk, J. W. *Phys. Rev.* **1981**, *24*, 1866.
(10) Nørskov, J. K.; Lundqvist, B. I. *Surface Sci.* **1979**, *89*, 251.
(11) Gadzuk, J. W. *Comm. At. Mol. Phys.* **1985**, *16*, 219.
(12) Brako, R.; Newns, D. M. *Rep. Prog. Phys.* **1989**, *52*, 655.
(13) Lundqvist, B. I. In *Electronic Processes at Solid Surfaces*; Ilisca, E., Makoshi, H., Eds.; World Scientific: Singapore, 1996; p 1.
(14) Grebor, T. *Surf. Sci. Rep.* **1997**, *28*, 1.
(15) Anderson, P. W. *Phys. Rev. Lett.* **1967**, *18*, 1049.
(16) Mahan, G. D. *Phys. Rev.* **1967**, *163*, 612.
(17) Nozières, P.; DeDominicis, C. T. *Phys. Rev.* **1969**, *178*, 1097.
(18) Hedin, L.; Lundqvist, S. *Solid State Phys.* **1969**, *23*, 1.
(19) Langreth, D. C. *Phys. Rev. B* **1970**, *1*, 471.
(20) Doniach, S.; Šunjic, M. *J. Phys. C* **1970**, *3*, 285.
(21) Mahan, G. D. *Solid State Phys.* **1974**, *29*, 75.
(22) Gadzuk, J. W.; Šunjic, M. *Phys. Rev. B* **1975**, *12*, 524.
(23) Gumhalter, B.; Newns, D. M. *Phys. Lett.* **1975**, *53A*, 137.
(24) Gunnarsson, O.; Schönhammer, K. *Phys. Rev. B* **1983**, *28*, 4315.
(25) *Many-Body Phenomena at Surfaces*; Langreth, D., Suhl, H., Eds.; Academic: Orlando, 1984.
(26) Kramer, J. *Z. Phys.* **1952**, *133*, 629.
(27) Gesell, T. F.; Arakawa, E. T.; Callcott, T. A. *Surf. Sci.* **1970**, *20*, 174.
(28) Cox, M. P.; Foord, J. S.; Lambert, R. M.; Prince, R. H. *Surf. Sci.* **1983**, *129*, 399.
(29) Böttcher, A.; Imbeck, R.; Morgante, A.; Ertl, G. *Phys. Rev. Lett* **1991**, *65*, 2035.
(30) Heilberg, L.; Strömquist, J.; Kasemo, B.; Lundqvist, B. I. *Phys. Rev. Lett.* **1995**, *74*, 4742.
(31) Oster, L.; Yaskolko, V.; Haddad, J. *Phys. Stat. Sol. (a)* **1999**, *174*, 431.
(32) Böttcher, A.; Niehus, H. *Phys. Rev. B* **2001**, *64*, 045407.
(33) Nienhaus, H.; Bergh, H. S.; Gergen, B.; Majumdar, A.; Weinberg, W. H.; McFarland, E. W. *Phys. Rev. Lett.* **1999**, *82*, 446.
(34) Nienhaus, H.; Bergh, H. S.; Gergen, B.; Majumdar, A.; Weinberg, W. H.; McFarland, E. W. *Surface Sci.* **2000**, *445*, 335.
(35) Gergen, B.; Weyers, S. J.; Nienhaus, H.; Weinberg, W. H.; McFarland, E. W. *Surface Sci.* **2001**, *488*, 123.
(36) Gergen, B.; Nienhaus, H.; Weinberg, W. H.; McFarland, E. W. *Science* **2001**, *294*, 2521.
(37) Auerbach, D. J. *Science* **2001**, *294*, 2488.
(38) Nienhaus, H. *Surf. Sci. Rep.* **2002**, *45*, 1.
(39) Gadzuk, J. W., to be published.
(40) Mead, C. A. *J. App. Phys.* **1961**, *32*, 646.
(41) Crowell, C. R.; Sze, S. M. *Phys. Thin Films* **1967**, *4*, 325.
(42) Lambe, J.; McCarthy, S. L. *Phys. Rev. Lett.* **1976**, *37*, 923.
(43) Wolf, E. L. *Principles of Electron Tunneling Spectroscopy*; Oxford: New York, 1985, p 352.
(44) Gadzuk, J. W. *Phys. Rev. Lett.* **1996**, *76*, 4234.
(45) Gadzuk, J. W. *J. Vac. Sci. Technol. A* **1997**, *15*, 1520.
(46) Bell, L. D.; Kaiser, W. J.; Hecht, M. H.; Davis, L. C. *Methods Experimental Phys.* **1993**, *27*, 307.
(47) Prietsch, M. *Phys. Repts.* **1995**, *253*, 163.
(48) de Andres, P. L.; Garcia-Vidal, F. J.; Reuter, K.; Flores, F. *Prog. Surface Sci.* **2001**, *66*, 3.
(49) Müller-Hartmann, E.; Ramakrishnan, T. V.; Toulouse, G. *Phys. Rev. B* **1971**, *3*, 1102.
(50) Brako, R.; Newns, D. M. *J. Phys. C: Solid State Phys.* **1981**, *14*, 3065.
(51) Gunnarsson, O.; Schönhammer, K. *Phys. Rev. B* **1982**, *25*, 2503.
(52) Stiles, M. D.; Hamann, D. R. *Phys. Rev. B* **1988**, *38*, 2021; Stiles, M. D.; Hamann, D. R. *Phys. Rev. B* **1989**, *40*, 1349.
(53) Pearson, D. A.; Sham, L. J. *Phys. Rev. B* **2001**, *64*, 125 408.
(54) Stiles, M. D., personal communication.
(55) Tersoff, J.; Hamman, D. R. *Phys. Rev. B* **1985**, *31*, 805.
(56) Methods of Experimental Physics In *Scanning Tunneling Microscopy*; Stroscio, J. A., Kaiser, W. J., Eds.; Academic: San Diego, 1993; Vol. 27.
(57) Quinn, J. J. *Phys. Rev.* **1962**, *126*, 1453; Quinn, J. J. *Appl. Phys. Lett.* **1963**, *2*, 167.
(58) Ohtaka, K.; Tanabe, Y. *Rev. Mod. Phys.* **1990**, *62*, 929.
(59) Hedin, L. *J. Phys.: Condens. Mater* **1999**, *11*, R489.
(60) Gadzuk, J. W. *J. Elec. Spectrosc. Relat. Phenom.* **1999**, *98*−*99*, 321.
(61) Tully, J. C.; Preston, R. K. *J. Chem. Phys.* **1971**, *55*, 562.
(62) Kleyn, A. W.; Los, J.; Gislason, E. A. *Phys. Rept.* **1982**, *90*, 1.
(63) Gadzuk, J. W.; Nørskov, J. K. *J. Chem. Phys.* **1984**, *81*, 2828.
(64) Holloway, S.; Gadzuk, J. W. *J. Chem. Phys.* **1985**, *82*, 5203.
(65) Gadzuk, J. W. *J. Chem. Phys.* **1987**, *86*, 5196.
(66) Los, J.; Geerlings, J. J. C. *Phys. Rept.* **1990**, *190*, 133.
(67) Tully, J. C. *J. Chem. Phys.* **1990**, *93*, 1061.
(68) Darling, G. R.; Holloway, S. *Rep. Prog. Phys.* **1995**, *58*, 1595.
(69) Bahim, B.; Teillet-Billy, D.; Gauyacq, J. P. *Surf. Sci.* **1999**, *431*, 193.
(70) Bach, C.; Groβ, A. *J. Chem. Phys.* **2001**, *114*, 6396.
(71) Ramakrishna, S.; Willig, F.; May, V. *J. Chem. Phys.* **2001**, *115*, 2743.
(72) Kleyn, A. W.; Moutinho, A. M. C. *J. Phys. B: At. Mol. Opt. Phys.* **2001**, *34*, R1.
(73) Nourtier, A. *J. Phys. (Paris)* **1977**, *38*, 479.
(74) Persson, B. N. J.; Persson, M. *Solid State Comm.* **1980**, *36*, 175.
(75) Schönhammer, K.; Gunnarsson, O. *Phys. Rev. B* **1983**, *27*, 5113.
(76) Head-Gordon, M.; Tully, J. C. *J. Chem. Phys.* **1992**, *96*, 3939.
(77) Persson, B. N. J. *Phys. Rev. B* **1993**, *48*, 18 143.
(78) Liebsch, A. *Phys. Rev. B* **1997**, *55*, 13 263.
(79) Persson, B. N. J.; Gadzuk, J. W. *Surface Sci.* **1998**, *410*, L779.
(80) Plihal, M.; Langreth, D. C. *Phys. Rev. B* **1999**, *60*, 5969.
(81) Tully, J. C. *Annu. Rev. Phys. Chem.* **2000**, *51*, 153.